Scanning Electrochemical Microscopy. 33. Application to the Study of ECE/DISP Reactions

Christophe Demaille,[†] Patrick R. Unwin,*[,‡] and Allen J. Bard*[,†]

Department of Chemistry and Biochemistry, The University of Texas at Austin, Austin, Texas 78712, and Department of Chemistry, University of Warwick, Coventry CV4 7AL, U.K.

Received: April 18, 1996[⊗]

The scanning electrochemical microscope (SECM) is used to measure the kinetics of ECE/DISP type reactions. The theory of the steady-state feedback response is developed in terms of numerical simulation. The theoretical curves show that the variation of the tip and substrate current with the tip−substrate separation can readily be used to differentiate between an ECE and a DISP1 pathway. The theoretical results suggest that rate constants up to 1.6×10^5 s^{-1} can be measured with tip sizes usually employed in SECM. The theory is validated using the experimental example of the reduction of anthracene in DMF in the presence of phenol. The reaction is shown to follow a DISP1 pathway, in agreement with previous studies. Good agreement is found between theory and experiment for all the phenol concentrations explored, and a rate constant of $(4.4 \pm 0.4) \times 10^3$ M^{-1} s^{-1} has been determined for the protonation of the anthracene radical anion by phenol.

Introduction

Previous work[1−5] has shown that the scanning electrochemical microscope (SECM) can be used as an efficient tool for studying the kinetics and mechanism of reactions following electron transfer. First-order[1] (EC) and second-order[2,4,5] (EC_{2i}) reactions were studied using this technique. The aim of this paper is to extend the use of SECM to the study of reactions in which two electrons are transferred. These reactions can be represented globally by the following scheme (written here for a cathodic process):

$$\text{electrode:} \quad A + e^- \rightarrow B \tag{1}$$

$$\text{solution:} \quad B \xrightarrow{k} C \tag{2}$$

$$\text{electrode:} \quad C + e^- \rightarrow D \tag{3}$$

The first electron transfer occurs at the electrode and leads to the species B that reacts in a first-order process to produce C. Very often C is easier to reduce than the starting material and undergoes a fast reduction. This second electron transfer can occur at the electrode as represented by reaction 3, but one also has to consider the following disproportionation reaction:[6]

$$\text{solution:} \quad C + B \xrightarrow{k_d} A + D \tag{4}$$

This results in the regeneration of A, which is then reduced at the electrode, leading also to an overall two-electron process.

The first limiting situation, corresponding to the second electron being transferred only via the reduction of C at the electrode, is denoted as an ECE type reaction. The second limiting situation, corresponding to the second electron being transferred only through the reduction of the regenerated A molecule, is said to be of the DISP type. Very often the difference in reduction potential between the A/B couple and the C/D couple is so large that the disproportionation reaction is diffusion-controlled. In this case, reaction 2 is then the rate-determining step and the scheme is of the DISP1 type.[7,8]

In this paper, we discuss the ability of the SECM to discriminate between the ECE and DISP1 pathways, and we develop the theory that will allow determination of the kinetic constant *k* from the SECM response. This theory is validated experimentally.

The principle behind the use of the feedback and generation/collection modes of the SECM for measuring coupled homogeneous chemical reactions has been discussed in great detail.[1,2] For the study of the ECE/DISP process, the potential of the tip ultramicroelectrode (UME) is scanned from a potential where A is not electroactive to a potential where the reduction of A is diffusion-controlled. The substrate is held at a potential where the oxidation of B is diffusion-controlled. Ideally, this potential corresponds to the foot of the wave for the reduction of A at the substrate. As mentioned previously, C is more easily reducible than A and its reduction at the tip (considered only in the case of the ECE pathway) is therefore also diffusion-controlled.

The assumption that C is much easier to reduce than A demands that, when the substrate potential is not very positive of the A/B wave, we consider the reduction of C *also* at the substrate electrode to be at a diffusion-controlled rate such that the processes occurring at the substrate are as follows:

$$\text{substrate:} \quad B - e \rightarrow A \quad \text{(ECE/DISP1)} \tag{5}$$

$$\text{substrate:} \quad C + e \rightarrow D \quad \text{(ECE pathway only)} \tag{6}$$

The diffusional and chemical processes occurring within the tip−substrate domain in the case of an ECE and a DISP1 pathway are shown schematically in Figure 1. A competition is established between the diffusion of B to the substrate (leading to the feedback of A to the tip) and the first-order chemical reaction (eq 2). At larger tip−substrate separations the coupled chemical reaction occurs. The apparent number of electrons transferred is then between 1 and 2, depending on the relative values of the kinetic constant *k* and the characteristic diffusion time of the UME (expressed by a^2/D, where *a* is the electrode radius and *D* the diffusion coefficient of A).[9] When the electrode is brought closer to the substrate, the presence of the substrate first results in the hindered diffusion of A to the tip, which diminishes the tip current. At very close tip−substrate

[†] University of Texas.
[‡] University of Warwick.
[⊗] Abstract published in *Advance ACS Abstracts,* August 1, 1996.

S0022-3654(96)01138-0 CCC: $12.00

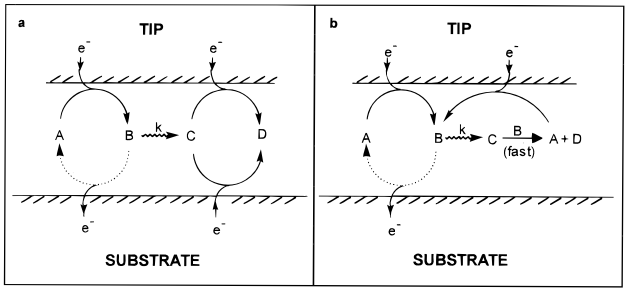

Figure 1. Diffusional and chemical processes occurring within the tip−substrate domain in the case of (a) an ECE pathway and (b) a DISP1 pathway.

separation, when the diffusion time of B across the gap (expressed as d^2/D, where d is the tip−substrate spacing) is small compared to its lifetime, the substrate regenerates A, which results in an increase of the tip current. The observation of the transition between those two regimes allows the determination of the kinetic rate of the homogeneous reaction.

It is also evident from Figure 1 that the measurement of the substrate current in the generation/collection mode, in addition to the tip current, provides a potential route to discriminating between the two mechanisms, since the conversion of C to D at the substrate in the ECE mechanism causes a cathodic current to flow.

The theory for the ECE/DISP1 problem is developed by extending the alternating direction implicit (ADI) finite difference method, which allows the numerical calculation of the tip and substrate currents as functions of (normalized) time, kinetic constant, and tip−substrate separation, following a potential step at the tip sufficient to cause the diffusion-controlled electrolysis of A. The experimental system of the reduction of anthracene in the presence of phenol in DMF is used to validate the theory and to demonstrate the applicability of the SECM feedback experiments for the study of two-electron reactions.

Theory

Formulation of the Problem. This paper is mainly concerned with the application of steady-state generation/collection measurements to the resolution of the ECE/DISP1 problem. However, since the ADI finite difference method[10] employed to provide a numerical solution to the problems of interest is an iterative procedure, we consider the case of potential step chronoamperometry and derive the steady-state characteristics from the long time behavior. This approach allows us to determine whether the transient measurements provide any additional information to steady-state measurements.

DISP1 Mechanism. The relevant time-dependent diffusion equations for this case, appropriate to the axisymmetric cylindrical SECM geometry, are

$$\frac{\partial c_A}{\partial t} = D_A\left[\frac{\partial^2 c_A}{\partial r^2} + \frac{1}{r}\frac{\partial c_A}{\partial r} + \frac{\partial^2 c_A}{\partial z^2}\right] + kc_B \qquad (7)$$

$$\frac{\partial c_B}{\partial t} = D_B\left[\frac{\partial^2 c_B}{\partial r^2} + \frac{1}{r}\frac{\partial c_B}{\partial r} + \frac{\partial^2 c_B}{\partial z^2}\right] - 2kc_B \qquad (8)$$

where r and z are the coordinates in the directions radial and normal to the tip electrode, respectively, starting at the center of the electrode surface. D_i and c_i are the diffusion coefficient and the concentration of species i (i = A or B), and t is time. The corresponding boundary conditions for the situation where reaction 1 is driven at a diffusion-controlled rate on the tip and reaction 5 occurs at a diffusion-controlled rate on the substrate electrode are

$$z = 0,\ 0 \le r \le a: \quad c_A = 0,\ D_A\frac{\partial c_A}{\partial z} = -D_B\frac{\partial c_B}{\partial z} \qquad (9)$$

$$z = 0,\ a < r \le r_g: \quad D_A\frac{\partial c_A}{\partial z} = D_B\frac{\partial c_B}{\partial z} = 0 \qquad (10)$$

$$z = d,\ 0 \le r \le r_g: \quad c_B = 0,\ D_B\frac{\partial c_B}{\partial z} = -D_A\frac{\partial c_A}{\partial z} \qquad (11)$$

$$r > r_g,\ 0 \le z \le d: \quad c_A = c_A^*,\ c_B = 0 \qquad (12)$$

$$r = 0,\ 0 < z < d: \quad D_A\frac{\partial c_A}{\partial r} = D_B\frac{\partial c_B}{\partial r} = 0 \qquad (13)$$

In eqs 9−13, a is the tip electrode radius, r_g is the radius of the disk-shaped tip end (electrode and surrounding glass insulator), and c_A^* is the concentration of A in bulk solution. The assumptions underlying the various boundary conditions for SECM problems have been delineated in earlier papers.[1,2,11] As in the previous treatment of the generation/collection mode,[2] it should be noted that in eq 11, it is assumed that the radius of the substrate electrode, r_s, is at least the magnitude of r_g. For the values of RG = r_g/a and tip−substrate separations appropriate to this study, this ensures the maximum collection efficiency such that, in the absence of homogeneous kinetic complications, all of the species B generated at the tip is collected at the substrate electrode.[2]

The initial condition completing the definition of the problem is

$$t = 0, \text{ all } r, \text{ all } z: \quad c_A = c_A^*,\ c_B = 0 \qquad (14)$$

The aim of the calculation is to determine the tip and substrate currents as a function of time, tip−substrate separation, and kinetics. The tip and substrate currents are evaluated, respectively, from

$$i_T = 2\pi F D_A \int_0^a (\partial c_A/\partial z)_{z=0} r\, dr \qquad (15)$$

$$i_S = 2\pi F D_B \int_0^{r_s} (\partial c_B/\partial z)_{z=d} r\, dr \qquad (16)$$

where F is the Faraday.

ECE Mechanism. The diffusion equations for species A, B, and C that have to be considered for this case are

$$\frac{\partial c_A}{\partial t} = D_A\left[\frac{\partial^2 c_A}{\partial r^2} + \frac{1}{r}\frac{\partial c_A}{\partial r} + \frac{\partial^2 c_A}{\partial z^2}\right] \qquad (17)$$

$$\frac{\partial c_B}{\partial t} = D_B\left[\frac{\partial^2 c_B}{\partial r^2} + \frac{1}{r}\frac{\partial c_B}{\partial r} + \frac{\partial^2 c_B}{\partial z^2}\right] - kc_B \qquad (18)$$

$$\frac{\partial c_C}{\partial t} = D_C\left[\frac{\partial^2 c_C}{\partial r^2} + \frac{1}{r}\frac{\partial c_C}{\partial r} + \frac{\partial^2 c_C}{\partial z^2}\right] + kc_B \qquad (19)$$

For conditions where reactions 1 and 3 are driven at a diffusion-controlled rate at the tip and reactions 5 and 6 occur at a diffusion-controlled rate at the substrate, the boundary

conditions are

$$z = 0,\ 0 \le r \le a: \quad c_A = 0,\ D_A\frac{\partial c_A}{\partial z} = -D_B\frac{\partial c_B}{\partial z},\ c_C = 0 \quad (20)$$

$$z = 0,\ a < r \le r_g: \quad D_A\frac{\partial c_A}{\partial z} = D_B\frac{\partial c_B}{\partial z} = D_C\frac{\partial c_C}{\partial z} = 0 \quad (21)$$

$$z = d,\ 0 \le r \le r_g: \quad c_B = 0,\ D_B\frac{\partial c_B}{\partial z} = -D_A\frac{\partial c_A}{\partial z},\ c_C = 0 \quad (22)$$

$$r > r_g,\ 0 \le z \le d: \quad c_A = c_A^*,\ c_B = 0,\ c_C = 0 \quad (23)$$

$$r = 0,\ 0 < z < d: \quad D_A\frac{\partial c_A}{\partial r} = D_B\frac{\partial c_B}{\partial r} = D_C\frac{\partial c_C}{\partial r} = 0 \quad (24)$$

The initial condition for potential step chronoamperometry is

$$t = 0, \text{ all } r, \text{ all } z: \quad c_A = c_A^*,\ c_B = 0,\ c_C = 0 \quad (25)$$

The tip and substrate currents (i_T and i_S) for the ECE process are now evaluated from

$$i_T = 2\pi F[D_A\int_0^a (\partial c_A/\partial z)_{z=0} r\, dr + D_C\int_0^a (\partial c_C/\partial z)_{z=0} r\, dr] \quad (26)$$

$$i_S = 2\pi F[D_B\int_0^{r_S} (\partial c_B/\partial z)_{z=d} r\, dr - D_C\int_0^{r_S} (\partial c_C/\partial z)_{z=d} r\, dr] \quad (27)$$

Solution of the Problem. To obtain general solutions, the problem was cast into dimensionless form by introducing the following dimensionless variables:

$$R = r/a \quad (28)$$

$$Z = z/a \quad (29)$$

$$C_i = c_i/c_A^* \quad (30)$$

$$\tau = tD/a^2 \quad (31)$$

$$K = ka^2/D \quad (32)$$

Equations 31 and 32 indicate that only the case where the participating species have equal diffusion coefficients, D, will be considered here.

Numerical solutions for the tip and substrate currents, normalized with respect to the kinetically uncomplicated one-electron steady-state current, which flows at infinite tip-substrate separation,[12]

$$i_{T,1e,\infty} = 4nFDac_A^* \quad (33)$$

were obtained using a Fortran or Pascal program based on the ADI finite difference method, which has been employed to solve previous SECM problems.[1−3] Treatment of the ECE and DISP1 generation/collection problem presents no additional conceptual difficulties from those outlined for electrode reactions involving first-order coupled chemical kinetics.[1]

Theoretical Results and Discussion

DISP1 Case. Typical steady-state tip and substrate currents corresponding to the DISP1 case are presented in Figure 2 for several values of the dimensionless kinetic parameter K. The tip current is normalized with respect to the uncomplicated diffusion-controlled current corresponding to the transfer of one electron. At infinite tip−substrate separation, the tip current depends on the relative values of the characteristic diffusion time in the stationary microelectrode diffusion layer (a^2/D) and the kinetic constant k. The dimensionless parameter K (eq 32) reflects the relative importance of those two parameters. For very small values of K, the tip current corresponds to the transfer of one electron. This corresponds to the situation where the electrode diameter is so small that the species B is taken away from the electrode vicinity by the spherical diffusion before it transforms into C, resulting in only one electron being transferred. In this situation there is nothing gained in approaching the tip to the substrate because the tip current would follow the upper dashed approach curve in Figure 2a. This corresponds to the pure diffusional feedback case, and no kinetic information could be deduced from the experiment. Therefore, when an unknown reaction is studied, the electrode radius should be sufficiently large that the approach curve significantly deviates from the kinetically uncomplicated diffusional feedback approach curve.

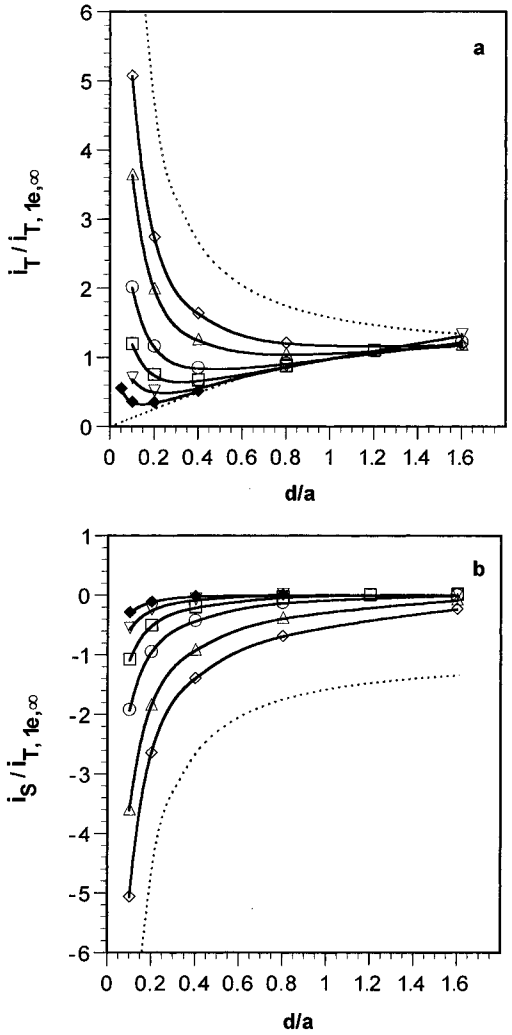

Figure 2. DISP1 pathway. Theoretical variation of the dimensionless tip and substrate currents with the tip−substrate dimensionless distance d/a for several values of $K = ka^2/D$: $K = 1$ (◇), 2 (△), 5 (○), 10 (□), 20 (▽), and 50 (◆). Part a shows the tip current, where the upper dashed line represents the one-electron pure positive feedback ($K = 0$). The lower dashed line represents the two-electron pure negative feedback ($K \to +\infty$). Part b shows the substrate current, where the dashed line represents the one-electron pure positive feedback.

As K approaches infinity, the electrode current at infinite tip−substrate separation corresponds to the transfer of two electrons.

In this case, when the tip approaches the substrate, the tip current decreases as a result of the hindered diffusion of A to the electrode surface. The approach curve is then identical to that corresponding to a two-electron pure negative feedback.

For intermediate values of K, the approach curve is located between the limiting curves corresponding to the one-electron positive feedback (upper limit at short tip−substrate separation) and the n-electron ($1 < n \leq 2$) negative feedback (lower limit at infinite tip−substrate separation). As the tip approaches the substrate, a competition is established between the diffusion of B across the gap and the rate of the homogeneous chemical reaction. This diffusion time is related to the tip−substrate distance rather than to the electrode radius and is defined by d^2/D. At very close tip−substrate separation (when $d^2/D \ll 1/k$) the flux of B leaving the electrode surface reaches the substrate surface before reacting, and it is therefore entirely converted into an equal flux of A that is fed back to the tip. The approach curve then tends toward the upper dashed curve corresponding to a pure one-electron positive feedback. The portion of the approach curve corresponding to the transition between the n-electron ($1 < n \leq 2$) negative feedback and the one-electron positive feedback contains the kinetic information. As can be seen in Figure 2a, such a transition can always be observed no matter how high the value of K if the tip−substrate distance is made small enough. However, in our experience, the minimum dimensionless tip−substrate separation routinely attainable is about $d/a = 0.2-0.1$. So evaluating the maximum kinetic constant that can be measured by the SECM technique in this case means evaluating the minimum deviation from the negative feedback behavior that can be observed for $d/a \approx 0.1$. From Figure 2a, one can estimate that this corresponds to about $K = 50$, so the maximum value of k measurable with an electrode of radius a is given by $k = 50D/a^2$.

Figure 2b presents the variation of the substrate current with the tip−substrate separation (i.e., a tip generation−substrate collection experiment). The main feature of this variation is that the substrate current remains equal to zero until the tip is close enough for species B to reach the substrate and be oxidized. The substrate current is therefore either equal to zero or of the opposite sign of the tip current. As the tip−substrate separation is made smaller, the substrate current tends toward the value corresponding to the one-electron positive feedback represented by the dashed line in Figure 2b.

ECE Case. Typical tip and substrate currents corresponding to the ECE case are presented in Figure 3. At long tip−substrate separation, the n-electron ($1 < n \leq 2$) tip current decreases with decreasing tip−substrate distance as a result of the hindered diffusion of A. In this part of the approach curve, the tip current for the ECE case is, however, always smaller than the one obtained in the DISP1 case for a given value of K, as illustrated in Figure 4. The reason for this is that, as shown in Figure 1, not only does species C diffuse back to the tip to exchange the second electron, but it can also exchange this second electron with the substrate, leading to an overall tip current that is smaller than the expected n-electron ($1 < n \leq 2$) negative feedback current (see Figure 4). This characteristic variation of the tip current with the tip−substrate distance can therefore be used to discriminate between an ECE and a DISP1 pathway. As in the DISP1 case, when the tip is brought closer to the substrate, the current tends toward the value corresponding to one-electron positive feedback.

Another particularly interesting consequence of the ability of C to be reduced at the substrate is that, for the ECE case, the substrate current changes sign as the tip−substrate separation decreases (see Figures 3 and 4). At long tip−substrate separation, the substrate current has the same sign as the tip current because the dominant electrochemical reaction at the substrate is the reduction of C. As the tip approaches the substrate, the oxidation of B occurs to a greater extent, and at a certain distance, these two currents cancel one another. At a shorter tip−substrate distance, the oxidation of B dominates and the substrate current is of the opposite sign to the tip current. One can therefore consider that the chemical reaction is "sensed" at a much greater tip−substrate separation in the ECE case through the production of the species C, which has, unlike in the DISP1 case, a long lifetime and must diffuse to one of the electrodes to be consumed. This change of sign of the substrate current is not observed in the DISP1 case and can therefore be used as a powerful experimental diagnostic to establish the occurrence of an ECE pathway.

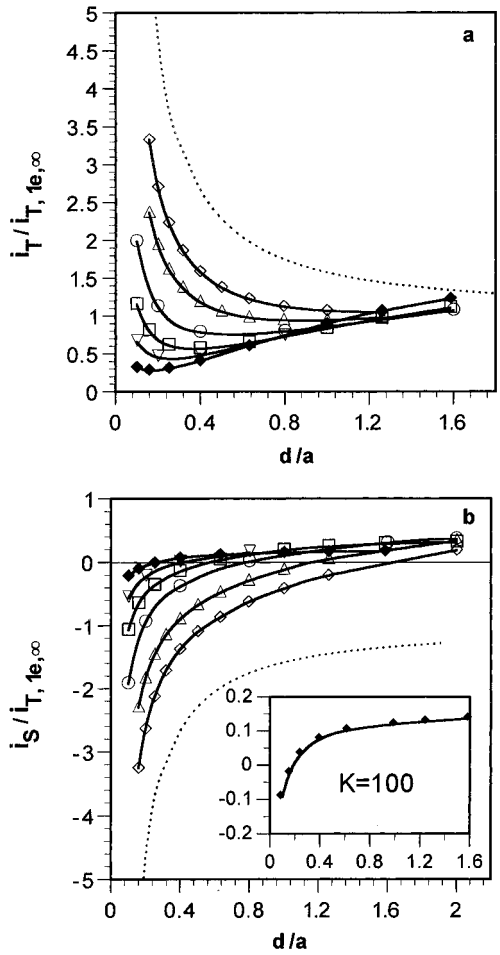

Figure 3. ECE pathway. Theoretical variation of the dimensionless tip and substrate current with the tip−substrate dimensionless distance d/a for several values of $K = ka^2/D$: $K = 1$ (◇), 2 (△), 5 (○), 10 (□), 20 (▽), and 50 (◆). Part a shows the tip current, where the upper dashed line represents the one-electron pure positive feedback ($K = 0$). Part b shows the substrate current, where the dashed line represents the one electron pure positive feedback. The inset shows the substrate current for $K = 100$.

From the approach curves presented in Figure 3, one can estimate that the maximum value of the chemical rate constant that is possible to measure in the ECE case is about the same as in the DISP1 case, ca. $k = 50D/a^2$. If the only purpose is to discriminate between an ECE and a DISP1 pathway, however, this can be achieved for much faster chemical reactions because, in the ECE case, the substrate consumes the species C at large tip−substrate separation, even for very large values of K (see the inset in Figure 3b, where even for $K = 100$, the substrate current is clearly greater than zero for $0.2 < d/a \leq 1.6$).

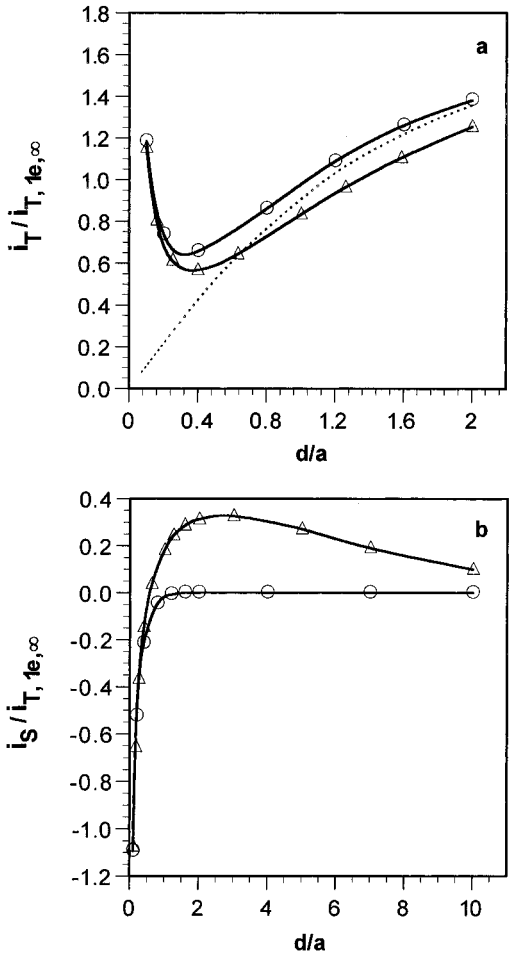

Figure 4. Comparison between the approach curves obtained for the DISP1 case (○) and the ECE case (△) for $K = 10$. Tip current (a) and substrate current (b) as a function of the dimensionless tip−substrate separation. The dashed curve in (a) represents the *n*-electron ($n = 1.7$) pure negative feedback current.

Range of Measurable Rate Constants. *Steady-State Characteristics.* The only practical limit to the maximum rate constant measurable using SECM is the distance of closest approach of the tip to the surface. This distance is related to the electrode size by physical constraints, such as the overall shape of the glass sheath or the tip−substrate alignment, which lead to an early contact of the insulator around the tip and prevent a further decrease in the tip−substrate distance. From an estimate of this distance of closest approach, ca. $d/a = 0.2-0.1$, the maximum electrode-radius-dependent rate constant for the ECE/DISP1 cases can be assigned as $k = 50D/a^2$. Assuming a diffusion coefficient of 10^{-5} cm^2 s^{-1} and by use of a 1-μm-diameter electrode, it would then be possible to measure rate constants as high as 1.6×10^5 s^{-1}. However, the fabrication of even smaller tips, e.g., carbon microdisk electrodes having a radius on the order of 0.1 μm[13] or even smaller Pt tips,[14] has been reported. If these electrodes proved to be suitable for SECM measurements, they would allow submicrosecond measurements under steady-state conditions.

Chronoamperometric Characteristics. Since the theoretical method adopted calculates the time-dependent response of the tip and substrate electrodes following a potential step at the tip sufficient to cause the diffusion-limited reduction of A, it is useful to consider briefly the type of information that transient methods can provide. In the fast kinetic limit, an ECE process can be identified unambiguously from the observation that a small substrate current flows that has the same sign as the tip current. Thus, it is particularly useful to determine to what extent this phenomenon applies in the time-dependent regime, since transient methods may increase the upper range of homogeneous rate constants accessible with SECM.[1]

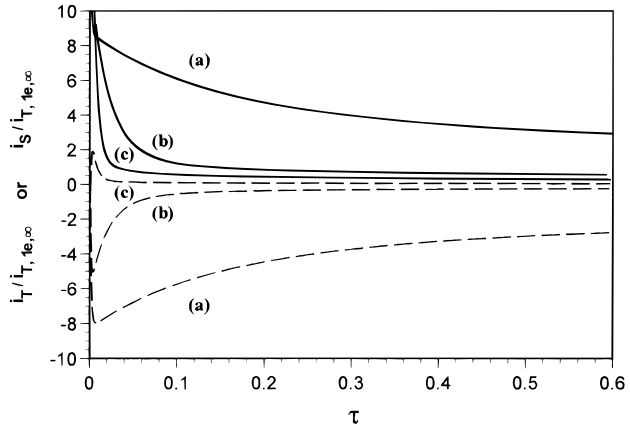

Figure 5. Tip (—) and substrate (- - -) current−dimensionless time characteristics for an ECE process with $d/a = 0.1$ and $K =$ (a) 10, (b) 100, and (c) 1000 ($\tau = Dt/a^2$).

Figure 5 shows the initial time dependence of the tip and substrate currents for an ECE process with $K = 10$, 100, and 1000 at $d/a = 0.1$. As the rate constant increases, the long-time tip current decreases for the reasons described above. However, at shorter times, $\tau < 0.005$, when the diffusion field at the tip electrode is much smaller than the tip−substrate separation, the tip current increases as the rate constant increases due to the homogeneous kinetics causing the electrode reaction to shift from one electron toward two electrons.

The long-time ($\tau \approx 0.5-0.6$) substrate currents re-emphasize the trend explained above for steady-state conditions as K increases: the current shifts from large values of sign opposite to that at the tip to very small values with the same sign as that at the tip. The same effect holds at short times, but the signal is significantly larger in the fast kinetic limit. In principle if times as short as $\tau \approx 0.01$ could be accessed experimentally, it should be possible to readily identify extremely rapid kinetics, up to $K \approx 1000$. However, for this particular case ($\tau K \approx 10$), this approach demands that measurements be made on a timescale of $\sim 10/k$, which may be difficult to achieve, since coupling between the tip and substrate responses can be significant at short times.

Experimental Results and Discussion

Reduction of Anthracene in DMF in the Presence of Phenol. In the presence of phenol, anthracene undergoes a two-electron reduction leading to 9,10-dihydroanthracene. This two-electron reduction follows a DISP1 pathway[8,15] and can be represented by the following reaction sequence:

$$A + e^- \rightleftarrows A^{\bullet -} \tag{34}$$

$$A^{\bullet -} + PhOH \xrightarrow{k'} AH^{\bullet} + PhO^- \tag{35}$$

$$AH^{\bullet} + A^{\bullet -} \xrightarrow{k_d} AH^- + A \tag{36}$$

$$AH^- + PhOH \xrightarrow{\text{fast}} AH_2 + PhO^- \tag{37}$$

$$A + 2e^- + 2PhOH \rightleftarrows AH_2 + 2PhO^- \quad \text{(overall)} \tag{38}$$

where A represents anthracene and PhOH, phenol.

In the presence of an excess of phenol, reaction 35 can be considered as a pseudo-first-order reaction. SECM experiments

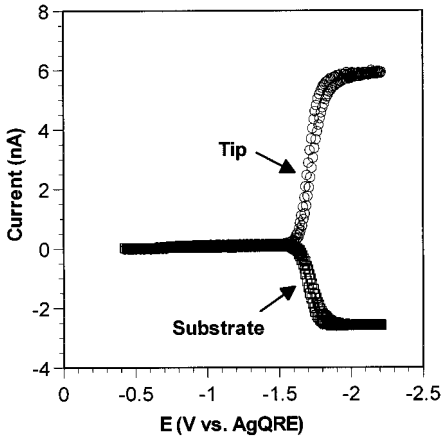

Figure 6. SECM voltammogram of anthracene (4.1 mM) in the presence of phenol (0.154 M) in DMF and 0.1 M $TBABF_4$ at a tip−substrate distance of $d/a = 0.22$. The tip was scanned at 50 mV/s. The substrate was a 60-μm-diameter gold disk held at a potential of −1 V vs AgQRE. Symbols represent the following: (○) tip current; (□) substrate current.

can therefore lead to the determination of the rate constant k' corresponding to the protonation of the anthracene radical anion by phenol. In a typical experiment, anthracene (4 mM), phenol (0.1−0.43 M), and supporting electrolyte ($TBABF_4$) were dissolved in DMF. The electrode was a 7 μm carbon ultramicroelectrode. The electrode size was selected so that at infinite tip−substrate separation the apparent number of electrons in the presence of the lowest phenol concentration was at least 1.5. Carbon was chosen as the electrode material because of the acidity of the medium, which would lead to ill-defined electrochemical response at metallic microelectrodes because of hydrogen evolution. Decamethylferrocene was also added to the solution and was used as a distance calibration mediator.[2,4,5] Experiments involved first recording the current corresponding to the oxidation of the mediator at infinite tip−substrate separation. The tip was then lowered toward the substrate until the desired value of the mediator positive feedback current was reached. This current value can be converted into a dimensionless tip−substrate distance d/a by using the theoretical diffusional positive feedback curves.[16] The microelectrode potential was then scanned in the negative direction, and the tip and substrate plateau currents for the reduction of anthracene were measured. Figure 6 shows typical voltammograms obtained. The tip current represents A and $AH^{\bullet}$ reduction, and the substrate current represents $A^{\bullet-}$ oxidation. The experiment was repeated for several tip−substrate separations (until the tip contacted the substrate surface) for each phenol concentration. The plateau currents were made dimensionless, using the value of the one-electron reduction of anthracene obtained in the absence of phenol, and were plotted as a function of the dimensionless tip−substrate separation d/a. Figure 7 shows a typical experimental approach curve obtained in this way.

The main feature of the experimental data is that the substrate current does not change sign with decreasing tip−substrate distance. This points to a DISP1 pathway, in agreement with results of previous work.[8,15] The point where substrate current begins to flow and positive feedback begins, at about $d/a = 0.4$, represents the point where $A^{\bullet-}$ begins to reach the substrate. The variation of the experimental tip currents as a function of the dimensionless tip−substrate distance recorded at several phenol concentrations is plotted in Figure 8. From the best fit between the experimental data and the theoretical approach curves, the value of K at each phenol concentration can be determined (see Figure 8). Since $K = ka^2/D = k'[\mathrm{PhOH}]a^2/D$,

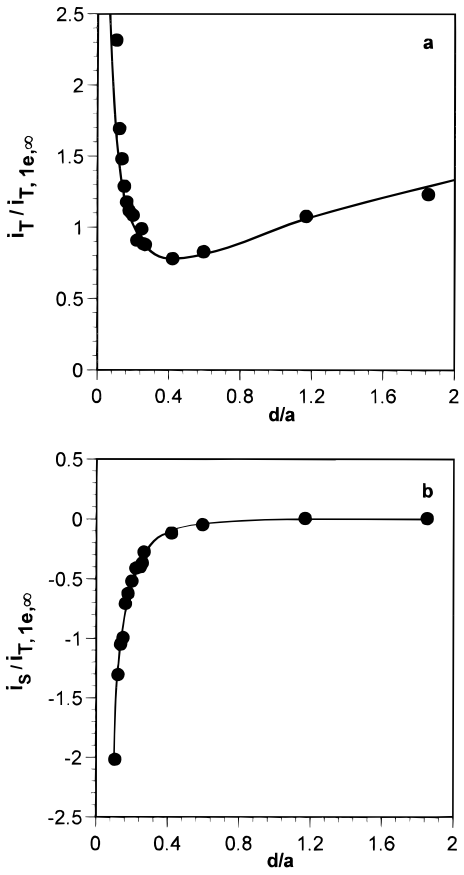

Figure 7. Reduction of anthracene (4.1 mM) in the presence of phenol (0.154 M) in DMF. Typical tip (a) and substrate (b) dimensionless currents measured at different tip−substrate separation.

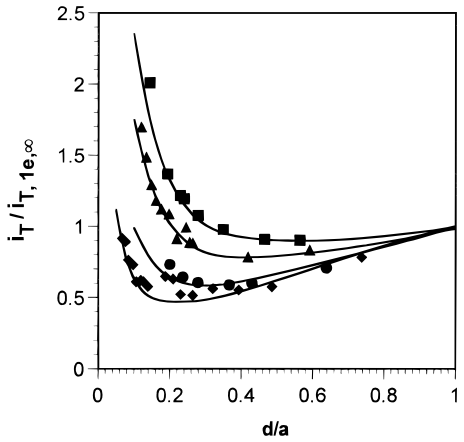

Figure 8. Normalized tip current as a function of the normalized tip−substrate distance for 0.1 (■), 0.154 (▲), 0.23 (●), and 0.43 (◆) M phenol, 4 mM anthracene, and 0.1 M $TBABF_4$ in DMF. The solid lines through each of the data sets indicate the best theoretical fit for the given value of K (from top to bottom $K = 4$, 6, 12.5, 22).

the value of K should be a linear function of the corresponding phenol concentration as shown in Figure 9. From the slope of this line, the value of the rate constant k' for the protonation of the anthracene radical anion (eq 35) can be determined if both the electrode radius and the diffusion coefficient of the anthracene are known. The electrode radius (3.5 μm) was measured optically under a microscope. The diffusion coefficient of anthracene was deduced from the value of the diffusion-limited current for the reduction of anthracene in the absence of phenol at infinite tip−substrate separation: $D = 1.07 \times 10^{-5}$ cm^2 s^{-1}. With these values, we determined the rate constant for the protonation of the anthracene radical anion by

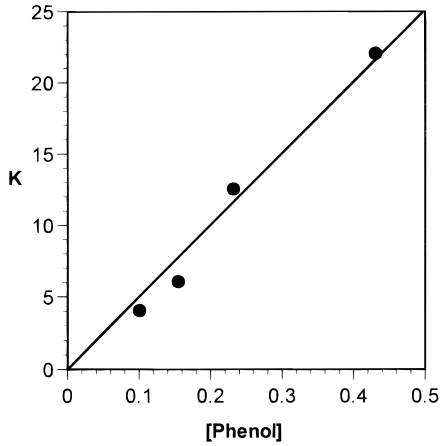

Figure 9. Experimental value of K as a function of the corresponding phenol concentration.

phenol to be $k' = (4.4 \pm 0.4) \times 10^3\ M^{-1}\ s^{-1}$. This value is in very good agreement with the value previously determined by Savéant and Amatore using double potential step chronoamperometry ($(4.8 \pm 0.8) \times 10^3\ M^{-1}\ s^{-1}$).[8]

Conclusions

This study has demonstrated that SECM can effectively be used to study the kinetics of two-electron chemical reactions. Not only can the kinetic constant of the rate-determining step be determined accurately, but the SECM can also be used to distinguish between ECE and DISP1 pathways. This makes the future studies of the many frequently observed two-electron reactions possible.

Experimental Section

Reagents. *N*,*N*-Dimethylformamide (DMF) (B&J Brand, Baxter, McGaw Park, IL) was stored in a dry box under a He atmosphere and was used without further treatment. Anthracene and phenol (Aldrich, Milwaukee, WI) were used as received. Decamethylferrocene (Strem, Newburyport, MA) was used without further purification. The supporting electrolyte, tetra-*n*-butylammonium tetrafluoroborate ($TBABF_4$, FLUKA, Buchs, Switzerland), was used as received.

Electrodes. Ultramicroelectrode tips were fabricated from 7-μm-diameter carbon fibers (Goodfellow, Cambridge, UK), as described previously.[16] For each electrode, the end of the glass sheath around the disk electrode was ground to yield a cone, and the tip was polished with alumina (down to 0.05 μm particle size). The electrode/glass radius ratio, *RG*, was close to 10 as measured optically. The substrate was a 60-μm-diameter gold electrode embedded in a glass sheath and placed in the base of the Teflon SECM cell. The substrate electrode was polished in the same way as the tips. A Pt wire was used as the counter electrode, and a Ag wire served as a quasi-reference electrode (AgQRE).

The solution was first purged of oxygen in a vial by bubbling argon for 15 min and then transferred by the argon pressure into the SECM cell through a small Teflon tube. Oxygen was kept out of the SECM cell by continuously flushing it with a gentle stream of argon. Control measurements determined that this did not result in a current increase due to unwanted convection. This procedure allowed the oxygen in solution to be kept at a negligible level throughout the experiment. The SECM instrument and electrochemical cell were described previously.[11]

Acknowledgment. The support of this work by grants from the National Science Foundation and the Robert A. Welch Foundation is gratefully acknowledged. This work has been facilitated by a NATO collaborative grant (CRG 941226), which we gratefully acknowledge. P.R.U. thanks the EPSRC for equipment support for the computations (GR/H61360).

References and Notes

(1) Unwin, P. R.; Bard, A. J. *J. Phys. Chem.* **1991**, *95*, 7814.
(2) Zhou, F.; Unwin, P. R.; Bard, A. J. *J. Phys. Chem.* **1992**, *96*, 4917.
(3) Unwin, P. R.; Bard, A. J. *J. Phys. Chem.* **1992**, *96*, 5035.
(4) Treichel, D. A.; Mirkin, M. V.; Bard, A. J. *J. Phys. Chem.* **1994**, *98*, 5751.
(5) Zhou, F.; Bard, A. J. *J. Am. Chem. Soc.* **1994**, *116*, 393.
(6) Hawley, M. D.; Feldberg, S. W. *J. Phys. Chem.* **1966**, *70*, 3459.
(7) Andrieux, C. P.; Savéant, J.-M. *J. Electroanal. Chem.* **1989**, *267*, 15.
(8) Amatore, C.; Gareil, M.; Savéant, J.-M. *J. Electroanal. Chem.* **1983**, *147*, 1, and references therein.
(9) Fleischmann, M.; Lasserre, F.; Robinson, J. *J. Electroanal. Chem.* **1984**, *177*, 115.
(10) Peaceman, D. W.; Rachford, H. H. *J. Soc. Ind. Appl. Math.* **1995**, *3*, 28.
(11) (a) Kwak, J.; Bard, A. J. *Anal. Chem.* **1989**, *61*, 1221. (b) Kwak, J.; Bard, A. J. *Anal. Chem.* **1989**, *61*, 1794.
(12) Saito, Y. *Rev. Polarogr.* **1968**, 15, 177.
(13) (a) Kim, Y. T.; Scarnulius, D. M.; Ewing, A. G. *Anal. Chem.* **1986**, *58*, 1782. (b) Wong, D. K. Y.; Xu, Y. F. L. *Anal. Chem.* **1995**, *67*, 4066.
(14) Fan, F.-R. F.; Bard, A. J. *Science* **1995**, *267*, 871.
(15) Amatore, C.; Savéant, J.-M. *J. Electroanal. Chem.* **1980**, *107*, 353.
(16) Bard, A. J.; Fan F.-R. F.; Kwak, J.; Lev, O. *Anal. Chem.* **1989**, *61*, 132.

JP9611380